Article

Temperature Distribution and Thermal Criticality of Kinetics Exothermic Reactant in Concentric Cylinders Subject to Various Boundary Conditions

Sulyman Olakunle Salawu [1],* and **Samuel Segun Okoya** [2]

1   Department of Mathematics, Bowen University, Iwo 232101, Nigeria
2   Department of Mathematics, Obafemi Awolowo University, Ile-Ife 220103, Nigeria
*   Correspondence: kunlesalawu2@gmail.com

Abstract: A study of the high-heat distribution of reacting species with approximation kinetics is essential in practical applications, for example, chemical synthesis, explosion safety and propulsion denotatives. As such, the temperature distribution and thermal criticality of an exothermic kinetics species in a concentric cylinder is the focus of this study. The chemistry of the pre-exponential factor, termination step, initiation rate and branch chain of the combustible reactant is investigated to study the system's critical behaviour. The temperature is assumed not to be large; as such, the consumption of reactant species is ignored. A partition weighted residual semi-analytical approximate solution to heat propagation under boundary conditions, thermal ignition and branch chain for varying activation energies and chemical kinetics is discussed. The solution validation criteria for the approximate semi-analytical method and numerical method are established. This study ascertained the impact of boundary conditions on the explosion, and the effect of certain parameter changes on the heat distribution and thermal criticality was shown to be significant. Hence, the outcomes offer an understanding into the homogeneous species behaviour in a cylindrical geometry.

Keywords: chemical kinetics; thermal ignition; initiation rate; branch-chain order

1. Introduction

Most of the combustion process involves heat evolution and distribution, and thermal ignition is noted when the exothermic heat generated by a reactive species is more than the ambient heat lost [1,2]. A study of the high-heat distribution of the oxidation of acetylene and hydrogen with approximation kinetics, which pertains to the diffusion or/and time history, is essential in practical applications, for example, chemical synthesis, explosion safety and propulsion denotatives. The thermal explosion theory of Frank–Kamenestskii assumes a stationary fuel mixture without reactant consumption, and the heat loss is based on the reactant mixture thermal conductivity and temperature gradient proportion, as presented by Ajadi and Goldshtein [3]. The study of Boddingtion et al. [4,5] was extended by Graham-Eagle et al. [6] to spheres and circular infinite cylinders for simultaneous endothermic and exothermic reactions, which resulted in the disappearance of criticality at low activation energies when using variational techniques. The values of the term that describes transition and criticality were comprehensively reported. Under reasonable physical assumptions, the disappearance of criticality and thermal criticality were accurately predicted (see [5,7,8]). It is worth noting that the critical conditions outlined above provide the criteria for safety requirements when handling and storing reactant species.

The highest-value λ_{cr} describe thermal criticality, a requirement for determining the exothermic materials' reaction safety. A chemical systems analysis of a classical phase of the thermal criticality branched-chain was conducted by [9–11]. Soon after, Varatharajan and Williams [9] considered the temperature distribution of a reactant undergoing heat exchange in an adiabatic vessel, using an asymptotic Frank–Kamenetskii high activation

energy limit to determine the explosion times' expression. However, less attention has been paid to the branch-chain thermal ignition of ambient heat loss [7,12]. Semenov [13] provided an analytical solution for the thermal ignition of exothermic species reactions with heat loss. The heat exchange Newton's law was assumed for the classical model, and an explosion branch-chain was obtained. A maximum temperature greater than the temperature of the critical ignition was shown to lead to the reactant's thermal explosion. For more information on the mathematical formulations, combustion characteristics, efficient solution techniques and various physical phenomena exhibited by exothermic reactant species, see [2,14–18].

The study of reactive or non-reactive species mixtures in an oriented concentric cylinder with isothermal or non-isothermal boundary conditions under reasonable physical conditions is a current research focus due to their industrial uses. Related studies can be seen in [19–21]. In a numerical study, the ignition behaviour of a non-premixed multiple burner was examined in a concentric combustion cylinder chamber by Machover and Mastorakos [22]. To avoid explosion, parameters that are sensitive to increases in temperature must be monitored. Shonhiwa and Zaturski [23] considered the thermal criticality disappearance for a viscous reactive material in an isothermal concentric cylinder. The transition, thermal explosion and criticality were extensively considered in their studies. Okoya [24] examined the ignition and criticality of nonlinear viscous reactive species material in an annular axial device. The Frank–Kamenetskii term and maximum temperature were shown to be influenced by the kinetic reactant, activation energy and material term. Yaseen et al. [25] discussed the Fakner–Skan wedge thermal nano-aggregation. Their outcomes established that thermal advancement is encouraged. Das et al. [26] reported on the thermal migration of tiny reactive particles in a concentric cylinder. Their findings showed that temperature distribution is significantly enhanced as the tiny particle interactions increase. Stolin et al. [17] investigated the thermal ignition of power-law hydromagnetic species in a concentric cylinder. Their report shows that the magnetic field dragged the reaction mixture. Okoya and Ajadi [7] analyzed the thermal condition equations of critical parameters using a concentric cylinder. It was ascertained that the boundary conditions influenced the explosion of reactive species.

Although there have been many studies on the behavior of various reactive materials in a cylinder, the temperature distribution and thermal criticality of kinetics exothermic reactants in a concentric cylinder subject to various boundary conditions have not been examined. As a result, the potential relevence of this study to oil exploration, fire safety, petrochemical industries and other industries motivated the current investigation. The present investigation used to the thermal explosion classical model of Varatharajan and Williams [9] under reasonable assumptions. Therefore, the study focuses on examining the impact of branch reaction order and initiation rate on the temperature distribution and criticality of kinetic exothermic reactions in a concentric cylinder. This study will increase the understanding of the effect of boundary conditions on thermal explosions, and the influence of parameter variations on the heat propagation and criticality of reactive materials.

2. The Basic Model Equations

Consider an innovative modification and extension of [9,11] a thermal explosion, branched-chain model describing the chemistry of a highly reactive ignition time mixture at rest in an infinite cylinder. The explosion branched-chain included termination steps, Arrhenius reaction rate, branched-chain order and initiation rate. A highly exothermic reaction was assumed, and up to a high ignition temperature time, no reactants consumption occurred. The combustible gas mixture of a spatially homogeneous reaction was established in a nonadiabatic system. The applications and limitations of the study are explained by Zeldovich et al. [14].

With pre-exponential index m, a generalized Arrhenius kinetics was assumed for the branched-chain term with activation energy E, as presented by Salawu et al. [2,15].

$$A = A_0 \left(\frac{k\bar{T}}{v\hbar} \right)^m \exp\left(-\frac{E}{R\bar{T}} \right). \tag{1}$$

A pure approximated diffusion reactive species of reduced order was considered according to Aleksandrov et al. [16]. Hence, the H equation balance takes the form

$$\frac{d[B]}{dt} = A[B]^n + \phi t + x\nabla^2[B]. \tag{2}$$

The initiation rate ϕt was chosen to be constant during ignition; with a suitable approximation, appropriate temperature-dependent initiation steps could be used, as follows:

$$C_2H_2 + O_2 \rightarrow CH_2CO + O, \ \ H_2 + O_2 \rightarrow H + HO_2.$$
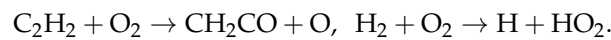
To obtain the kinetic balance (2), a term denoting particle diffusion was added under the species gradient to prevent the wall absorption of active species, as defined by Semenov [13]. Therefore, the system conservation of energy resulted in a linearly dependent temperature for the species concentration, in accordance with the work of Zeldovich et al. ([14], p. 85). This can be shown as

$$\bar{T} = \bar{T}_0 + \delta[B]. \tag{3}$$

The generalized thermal explosion theory that characterized the energy conservation equation is described by [22,27] as:

$$x\nabla^2\bar{T} + \delta A_0 \left(\frac{k\bar{T}}{v\hbar} \right)^m \left(\frac{\bar{T} - \bar{T}_0}{\delta} \right)^n \exp\left(-\frac{E}{R\bar{T}} \right) + \delta\phi t = 0. \tag{4}$$

For physical interpretation and implications, the suitable boundary conditions for the reactive species in a concentric cylinder are given as in the work of Okoya [18]

$$\text{Case 1: Asymmetric conditions } \bar{T}(r_1) = \bar{T}_1 \ \text{ and } \ \bar{T}(r_2) = \bar{T}_2, \tag{5}$$

$$\text{Case 2: Mixed type 1 conditions } \bar{T}(r_1) = \bar{T}_1 \ \text{ and } \ \frac{d\bar{T}}{d\bar{r}}(r_2) = 0, \tag{6}$$

$$\text{Case 3: Mixed type 2 conditions } \frac{d\bar{T}}{d\bar{r}}(r_1) = 0 \ \text{ and } \ \frac{d\bar{T}}{d\bar{r}}(r_2) + B\bar{T}(r_2) = 0. \tag{7}$$

For a thermally insulated cylinder in an adiabatic thermodynamic process, Equation (4) has no solution for the boundary condition

$$\bar{T}'(r_1) = 0 \ \text{ and } \ \bar{T}'(r_2) = 0, \tag{8}$$

due to the heat dissipation that occurs without removal.

Here, the thermal and species effect were taken to be unidirectionally distributed, and both served as a function of $\bar{r}$. The parameters κ, $[B]$, k, δ, R, A_0, v, $\hbar$, n, $\bar{T}$, t, x and ∇ are, respectively, the diffusion coefficient, concentration of active species, Boltzmann constant, energy release per fuel mole, gas constant, generalized rate of branched-chain order, vibration frequency, Planck's constant, reaction branch order, temperature, time, diffusion coefficient and operator gradient.

The geometry of the species propagation in a cylinder is demonstrated in Figure 1. A $\bar{z}$-axis unidirectional distribution was assumed, such that the species is only a function of $\bar{r}$, and heat transfer within the system was slower than the ambient heat transfer for the nonadiabatic thermodynamic process. By eliminating the term $[B]$ from Equation (2)

through Equation (3), the dimensionless form of the quasilinear Equation (4) for the reactive species temperature was connected with [3,11,28]

$$\frac{d^2T}{dr^2} + \frac{1}{r}\frac{dT}{dr} + \gamma + \lambda T^n(1+\alpha T)^m \exp\left(\frac{T}{1+\alpha T}\right) = 0. \tag{9}$$

In Equation (9), the dimensionless terms T, γ, r, α and λ, respectively, represent the temperature, initiation rate, cylinder radius, activation energy and Frank–Kamenetskii. The boundary conditions in dimensionless terms can be described as follows:

$$\text{Case 1: Asymmetric dimensionless conditions} \quad T(h) = a \text{ and } T(1) = b, \tag{10}$$

$$\text{Case 2: Mixed type 1 dimensionless conditions} \quad T(h) = a \text{ and } \frac{dT}{dr}(1) = 0, \tag{11}$$

$$\text{Case 3: Mixed type 2 dimensionless conditions} \quad \frac{dT}{dr}(h) = 0 \text{ and } \frac{dT}{dr}(1) + BiT(1) = 0. \tag{12}$$

The following variables were used to obtain the dimensionless modeled Equations (9)–(12):

$$T = \frac{E(\bar{T} - \bar{T}_0)}{R\bar{T}_0^2}, h = \frac{r_1}{r_2}, r = \frac{\bar{r}}{r_2}, \gamma = \frac{\delta r_1^2 \phi t}{\bar{T}_0 \alpha x}, \lambda = \frac{\delta r_1^2 A_0 E}{x R \bar{T}_0^2}\left(\frac{\alpha \bar{T}_0}{\delta}\right)^n \left(\frac{k\bar{T}_0}{\nu \hbar}\right)^m \exp\left(-\frac{1}{\alpha}\right),$$

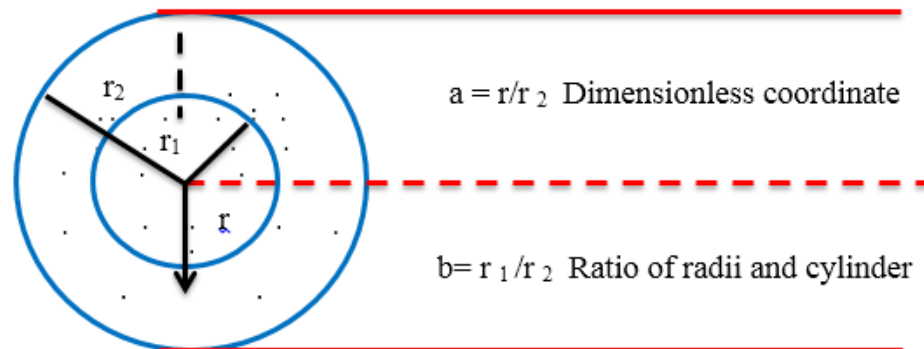$$\alpha = \frac{R\bar{T}_0}{E}, Bi = \frac{r_2 B}{k}.$$

Figure 1. Reaction species coordinate geometry.

Thus, the problems with such boundary conditions were previously investigated by Okoya and Ajadi [7]. Stolin et al. [17] investigated these problems for the case $m = n = \gamma = 0$, while Okoya [18] considered $n = \gamma = 0$. In special cases including a channel device without heat loss, Equation (9) was developed similarly to the work of Kurose and Makino [29], without n and α, and Okoya [12] in the absence of heat loss. The Frank–Kamenetskii [27] classical case is obtained when $\gamma = n = \alpha = 0$. However, when $\gamma \neq$ or $m = n = \gamma = 0$, the main equation reduces to Shonhiwa and Zaturska [23] or Ajadi [28] and Jha et al. [30]. The equation is also equivalent to Okoya [24] without flow momentum.

For a steady-state species premixed reaction, a constant exothermic combustible heat was released to the ambient temperature via the exterior wall. As such, a natural convect of the outer wall with the neighboring air exists, as reported in Junwei and Beijing [31]. Therefore, the temperature gradient at the outer wall could be used to denote the Nusselt number (Nu), which is essential to the engineering field. This is given in dimensionless form as follows:

$$Nu = -\left.\frac{dT}{dr}\right|_{r=1}. \tag{13}$$

3. Methods of Solutions

3.1. Semi-Analytical Method

The modeled exothermic species reaction with the boundary conditions of Equations (9)–(12) were analytically solved by the weighted residual technique, along with the partition integration method [32–34], to examine parameter sensitivity. Here, a polynomial trial function was assumed for the $T(r)$ in the temperature equation as follows:

$$T(r) = \sum_{i=0}^{n} g_i r^i, \tag{14}$$

where g_i is the constant to be determined and n is the fixed whole number.

As in the weighted residual solution procedure, a trial polynomial function was chosen to satisfy the boundary conditions. Therefore, conditions (10)–(12) were separately imposed on the Equation (14) to obtain a separate system of equations in terms of g_i.

The basis polynomial function was also used in Equation (9) to obtain the residual equation, which was then minimized to become as close as possible to zero.

$$
\begin{aligned}
T_{res}(r) = {} & 90\,r^8 g_{10} + 72\,r^7 g_9 + 56\,r^6 g_8 + 42\,r^5 g_7 + 30\,r^4 g_6 + 20\,r^3 g_5 + 12\,r^2 g_4 + 6\,r g_3 + 2\,g_2 + \\
& \frac{10\,r^9 g_{10} + 9\,r^8 g_9 + 8\,r^7 g_8 + 7\,r^6 g_7 + 6\,r^5 g_6 + 5\,r^4 g_5 + 4\,r^3 g_4 + 3\,r^2 g_3 + 2\,r g_2 + g_1}{r} + \gamma + \\
& \lambda \left(g_{10} r^{10} + g_9 r^9 + g_8 r^8 + g_7 r^7 + g_6 r^6 + g_5 r^5 + g_4 r^4 + g_3 r^3 + g_2 r^2 + g_1 r + g_0 \right)^n \times \\
& \left(\left(g_{10} r^{10} + g_9 r^9 + g_8 r^8 + g_7 r^7 + g_6 r^6 + g_5 r^5 + g_4 r^4 + g_3 r^3 + g_2 r^2 + g_1 r + g_0 \right) \alpha + 1 \right)^m \times \\
& \exp \left(\frac{g_{10} r^{10} + g_9 r^9 + g_8 r^8 + g_7 r^7 + g_6 r^6 + g_5 r^5 + g_4 r^4 + g_3 r^3 + g_2 r^2 + g_1 r + g_0}{(g_{10} r^{10} + g_9 r^9 + g_8 r^8 + g_7 r^7 + g_6 r^6 + g_5 r^5 + g_4 r^4 + g_3 r^3 + g_2 r^2 + g_1 r + g_0) \alpha + 1} \right).
\end{aligned}
\tag{15}
$$

A partition integration method was adopted for minimization in the boundary domain, which was subdivided into an arbitrary sub-domains as follows:

$$0 - r_1, r_1 - r_2, r_2 - r_3, \ldots, r_n - 1 \text{ where } 0 < r_1 < r_2 < r_3, \cdots < r_n < 1$$

Due to the direct integration's complexity, the obtained residual T_r was integrated within the sub-domain using one-third Simpson rule to obtain the system of equations in g_i's. The imposed boundary conditions for the trial function and the system of residual equations were simultaneously solved via Maple software to determine the constant g_i's. Hence, the constants were substituted into the trial function to obtain the required solution. Note that the system of equations must be in accordance with the number of constants in the trial function.

3.2. Results Presentation and Comparison

A partition integration scheme was coupled with the analytical weighted residual procedure to obtain the solutions to the exothermic species reaction in a concentric cylinder. Throughout the solution procedures, the default values were $m = \gamma = 0.5$, $\alpha = 0.2$, $n = 1.0$, $\lambda = 0.1$, $a = 1.0$, $b = 2.0$ and $h = 0.2$, unless otherwise indicated on each plot. In Table 1, the temperature gradient at the concentric cylinder wall for the asymmetric and mixed type 1 conditions is presented. The wall effect is very pronounced for the asymmetric conditions compared to the mixed type 1 conditions for various combustion terms, while the energy terms are shown to have no effect on the mixed type 2 conditions. As observed, the ambient heat transfer incresed when the natural outer wall convect was used as the thermo-parameters. As such, the outer wall heat gradient dominated the exothermic combustible species. In Table 2, the semi-analytical computed results are compared with the Runge–Kutta (R-K) numerical scheme. The absolute error of 10^{-6} shows a good qualitative and strong quantitative agreement between this solution technique and the numerical method.

Table 1. The concentric cylinder wall heat gradient for different conditions.

γ	λ	α	m	n	Asymmetric Conditions	Mixed Type 2 Conditions
0.5	0.1	0.2	0.5	1.0	0.142605760	0.826773598
0.7					0.068713729	0.939952662
	0.07				0.236601339	0.629676051
	0.15				0.020551671	1.220893443
		0.1			0.092234542	0.995247778
		0.3			0.173033013	0.743315791
			−2.0		0.312229943	0.460637107
			0.0		0.189263346	0.714959625
				0.3	0.253515080	0.561043255
				0.7	0.196972165	0.687664032

Table 2. The analytical and numerical outcomes' validation for mixed type 1 conditions.

h	PWRM $T(r)$ Outcomes	R-K Numerical $T(r)$ Outcomes	Absolute Error
0.2	1.000000000	1.000000000	0
0.3	1.200701962	1.200703920	1.96×10^{-6}
0.4	1.335717301	1.335744481	2.72×10^{-5}
0.5	1.432171360	1.432174785	3.43×10^{-6}
0.6	1.501899779	1.501899963	1.84×10^{-7}
0.7	1.551207219	1.551203670	3.55×10^{-6}
0.8	1.583825778	1.583822025	3.75×10^{-7}
0.9	1.602183557	1.602186780	3.22×10^{-6}
1.0	1.608005656	1.608005997	3.41×10^{-7}

3.3. Concentric Cylinder Heat Propagation of Reactive Specie

The heat distribution of exothermic species diffusion reactions in a concentric cylinder is presented for different boundary condition cases. The presented results are for the asymmetric boundary conditions, mixed type 1 dimensionless conditions and convective mixed type 2 boundary conditions, respectively.

Case 1: The results for the asymmetric boundary conditions.

The heat propagation in Figures 2 and 3 under asymmetric boundary conditions $T(h) = a$ and $T(1) = b$ were examined for variations in the initiation rate (γ) and Frank–Kamenetskii (λ). The initiation rate involves the translation of the exothermic heat generated by chemical reactions and species molecules in a reactive system, and measures the rate of chemical synthesis in a combustion system. An increasing initiation rate stimulated species' molecular synthesis, which increases heat propagation. The Frank–Kamenetskii term (λ) raises the temperature profile of homogeneous reactant mixtures when kept in a long concentric cylinder under asymmetric conditions. The effects of the reaction branch-chain (n) and reaction kinetics (m) on the species temperature are depicted in Figures 4 and 5. In Figure 4, a rapid reaction process producing the same products is initiated, leading to an increasing heat profile as the branch-chain is increased. The branch-chain reaction is very sensitive to the species mixture conditions, because the reactions sustain substances that are influenced by other substances, rather than the reactants themselves. As obtained in Figure 5, the species reaction rate increases with an increase in the chemical kinetics, which increases the temperature profile. This supports the chemical mechanism procedures of a reaction mixture, thereby propelling the heat distribution throughout the concentric cylinder.
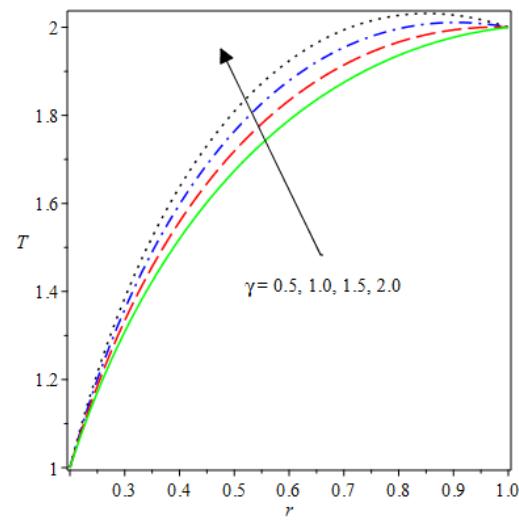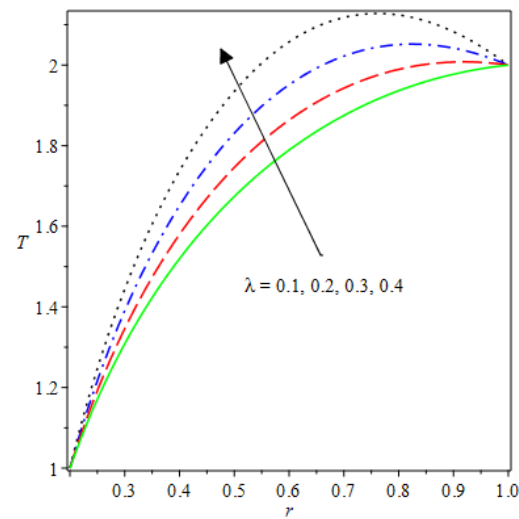
Figure 2. Heat distribution for varying (γ).

Figure 3. Temperature field for increasing (λ).
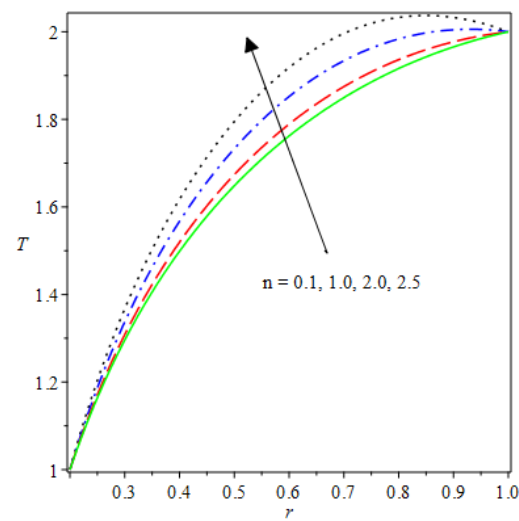

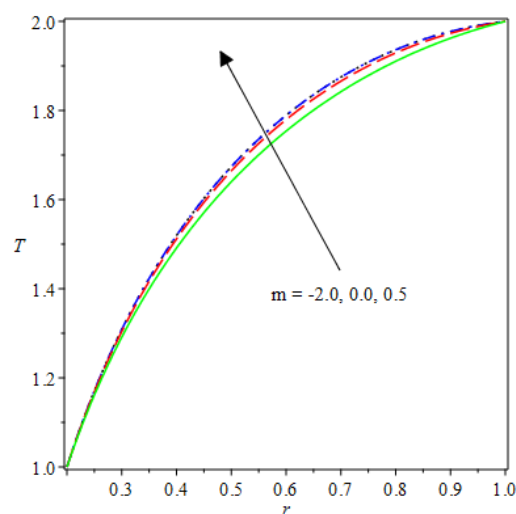**Figure 4.** Heat distribution for varying (n).

Figure 5. Temperature field for rising (m).

Case 2: Mixed type 1 boundary conditions.

Figures 6–9 demonstrate the impact of the mixed type 1 boundary conditions $T(h) = a$ and $T'(1) = 0$ on reactant heat propagation in a concentric cylinder. As shown in Figure 6, an increase in initiation rate (γ) enhances the temperature distribution along the cylinder medium. This is because the species mixtures is inspired by the early stimulation of activation energy that induces the interaction between free particles, encouraging internal heating. In Figure 7, the influence of the branch-chain reaction order is examined under conditions of heat transfer. The reaction branch-chain is a criterion for the thermal explosion of oxidative species at high temperatures. As displayed in Figure 7, the species reaction temperature is adiabatic in nature, resulting in exponentially increasing heat transfer as the species molecules are mixed with oxygen. This propels the increasing temperature distribution for the mixed type 1 boundary conditions. In Figure 8, the Frank–Kamenetskii parameter (λ) is a strong heat generation term, which propels the high-combustible-temperature distribution of chemical reactants. As a result, an increase in the term (λ) must be carefully watched to prevent combustible reactants from blowup. The heat transfer's response to the rising chemical kinetics (m) is displayed in Figure 9. The bimolecular kinetic has the highest heat generation, while the sensitized kinetic has the lowest heat generation strength. Hence, heat propagation and diffusion are propelled as the reaction kinetics increase.
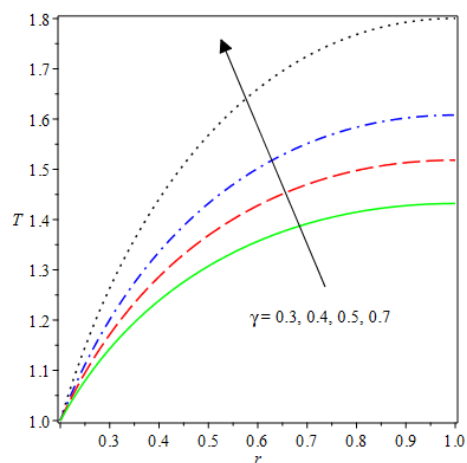

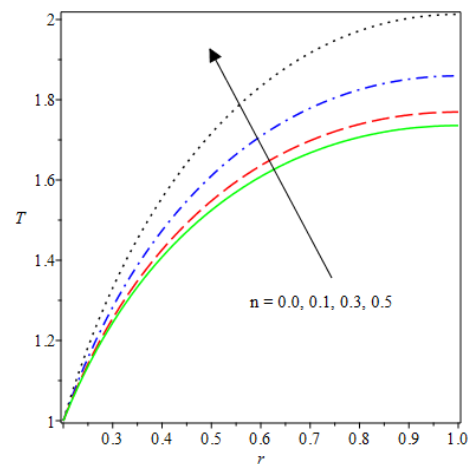**Figure 6.** Temperature profile for increasing (γ).
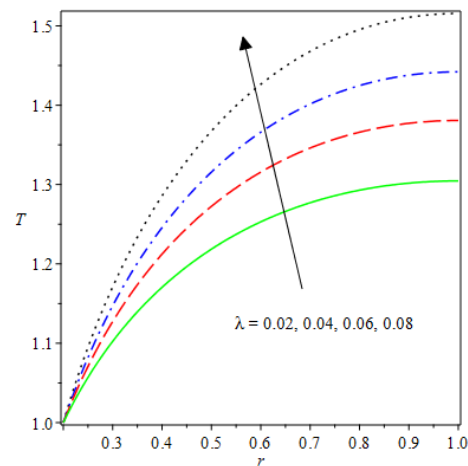
Figure 7. Heat transfer for different (n).

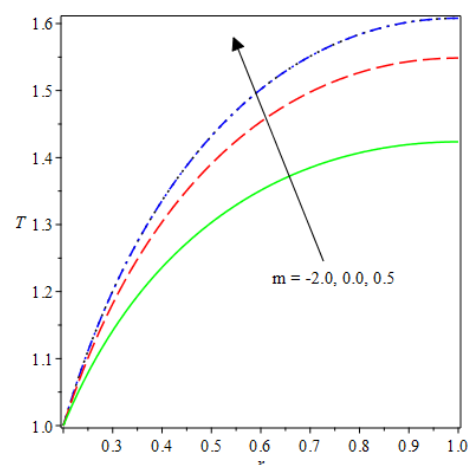**Figure 8.** Temperature profile for increasing (λ).

Figure 9. Heat transfer for different (m).

Case 3: Convective mixed type 2 boundary conditions.

The convective mixed boundary conditions' effect on the reacting species' temperature is demonstrated in Figures 10–15. The changes in the Frank–Kamenetskii term (λ), initiation rate (γ) and reaction kinetics (m) for the mixed conditions $T'(h) = 0$ and $T'(1) + BiT(1) = 0$ led to a significant rise in the temperature fields. The homogeneous

reactant mixtures of the thermal explosive species in the concentric cylinder increased at a constant wall temperature and density. This leads to a sharply increasing heat propagation with negligible reactant concentration consumption; hence, the parameters characterize reactant species' ignition. When the terms are high, the chemical reaction time is less than the heat conduction time; as such, at high temperatures, the system explodes. Therefore, as seen in Figures 10–12, parameters that encourage a high heat distribution with a high conduction time in a combustible system must be discouraged to avoid system explosion. Meanwhile, in Figures 13–15, rising branch-chain order (n), Biot number (Bi) and activation energy (α) reduce the temperature field due to a decrease in the thermal boundary film, allowing high ambient heat diffusion. This diminishes the heat content in the concentric cylinder; as such, the interaction between species molecules is damped. Hence, temperature distribution reduces as the convective heat cooling dominates the chemical reaction. During the cooling process, the heat leads to fluid expansion, which reduces the density and temperature profiles.
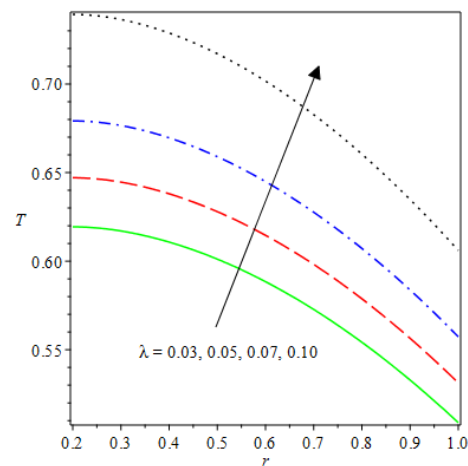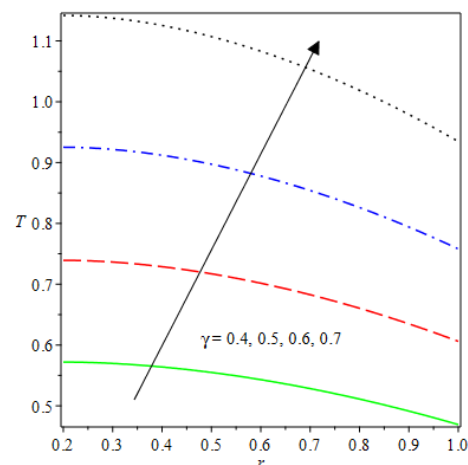

Figure 10. Temperature profile for rising (λ).

Figure 11. Heat transfer for different (γ).
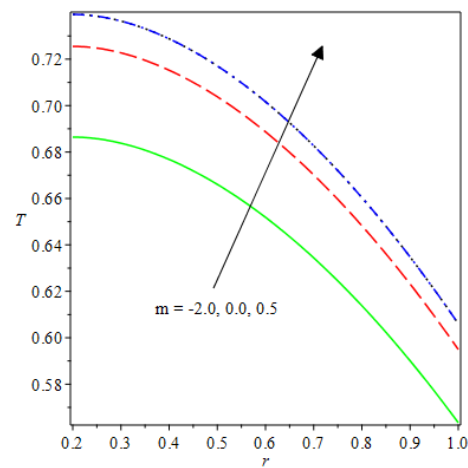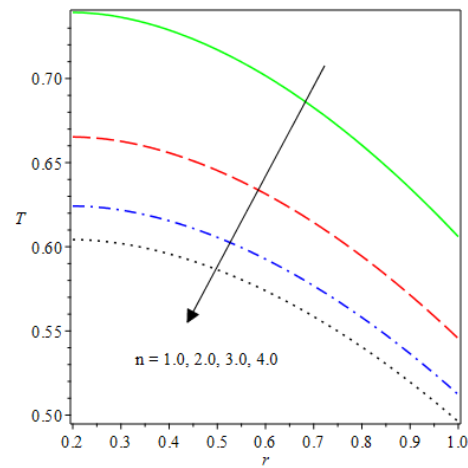
Figure 12. Temperature profile for rising (m).

Figure 13. Heat transfer for rising (n).
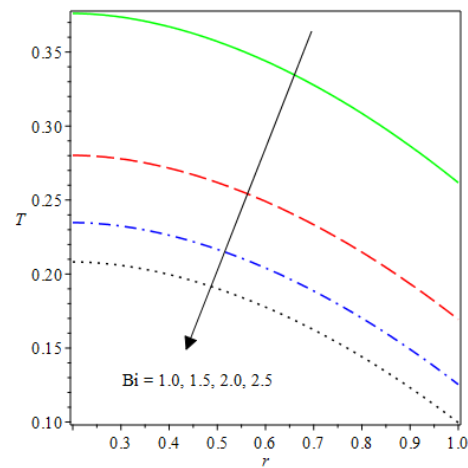

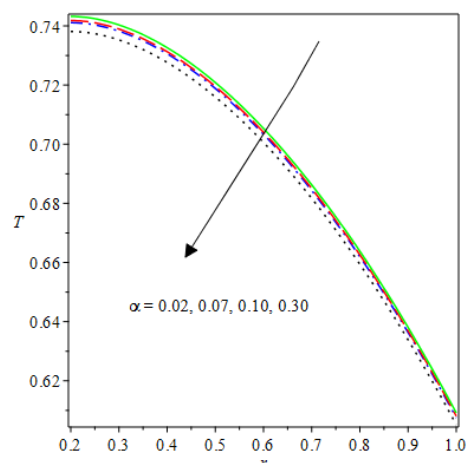**Figure 14.** Temperature profile for rising (Bi).

Figure 15. Heat transfer for rising (α).

4. Parameter-Dependent Thermal Criticality Bifurcation Solutions

A function $T_{max}(\lambda)$ describing the maximum temperature, T_{max}, as a function of the Frank–Kamenetskii term, λ, denoted thermal ignition. A sharp increase in the temperature gradient $dT_{max}/d\lambda$ is revealed when $\alpha = 0$. The maximum heat gradient that leads to detonation/explosion depends on the value of λ, which is the required condition for thermal criticality to occur. T_{max} is usually very sensitive to small variations in the initial conditions at the region near the λ_{cr}. Hence, the response to the initial temperature resulted in thermal criticality, which can also be obtained experimentally. Mathematically, $dT_{max}/d\lambda = 0$ is defined as the thermal criticality (or ignition/detonation) that produces λ due to the increasing T_{max}, which is asymptotic to the axis. The critical term depends on the geometry, and semi-analytical calculations are not trivial. The method provides the thermal explosion point, which can be extended to an explosion branch-chain that is identified as the reaction bifurcation point of the system from conditions (9) to (12).

4.1. Implementation of a Weighted Residual Analytical Solution

In this study, an analytical evaluation of the criticality bifurcation was carried out using the partition weighted residual analytical scheme, as explained in Section 3.1. A trial function, as defined in Equation (14), was assumed in terms of $T(r)$. This is applied to the boundary conditions (10)–(12) to obtain a modified $T(r)$ in the form $T(r)_{max}$. The obtained modified temperature maximum was substituted into the quasilinear Equation (9) and evaluated with the default values $m = \gamma = 0.5$, $\alpha = 0.2$, $n = 1.0$, $a = 1.0$, $b = 2.0$ and $h = 0.2$. Hence, a slice branch-chain diagram can be seen in the direction (λ, T_{max}) with critical value λ_{cr}, satisfying the range $0 \leq \lambda \leq \lambda_{cr}$. Therefore, the value of $(\lambda_{cr}, T_{max\,cr})$ = (0.578507, 1.591503) was obtained under asymmetric boundary conditions.

4.2. Ignition Slice and Thermal Runaway

The ignition bifurcation slice diagrams in the plane (λ, T_{max}), showing differences in activation energy (α) and kinetics reaction (m) values, are depicted in Figures 16 and 17 for the asymmetric boundary conditions. For $0 \leq \alpha << 1$ and various kinetics within the range $0 < \lambda < \lambda_{cr}$, the critical value λ_{cr} was found. Two results were obtained, the lower stable branches and upper branches diverged to infinity. No real outcome regarding the species reaction when $\lambda_{cr} < \lambda$ was obtained, excepting a traditional one denoting criticality. The thermal criticality increases with rising activation energy, but reduces with the kinetics reaction, as shown in Figures 16 and 17. A momentous change in the criticality λ_{cr} and maximum heat $T_{max\,cr}$ for species combustion in a concentric cylinder under increasing (α) and (m) is displayed in Figures 18 and 19. A variation in the branching order (n) leads to a decrease in the species exothermic mixture of homogeneous reactants under mixed type

1 concentric boundary conditions. This demonstrates the reduction in the early thermal runaway formation as a result of ambient exothermic heat propagation.
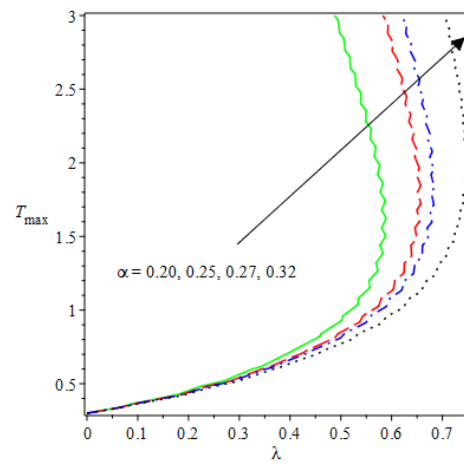
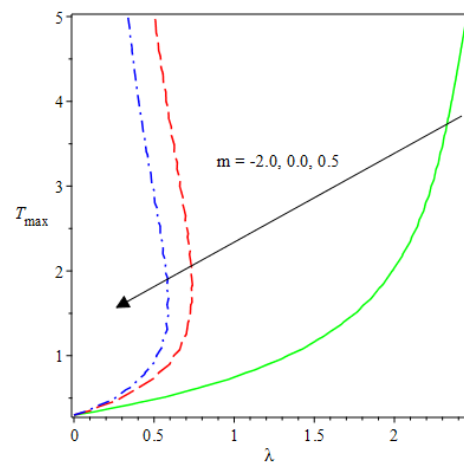**Figure 16.** Bifurcation slice for various (α).
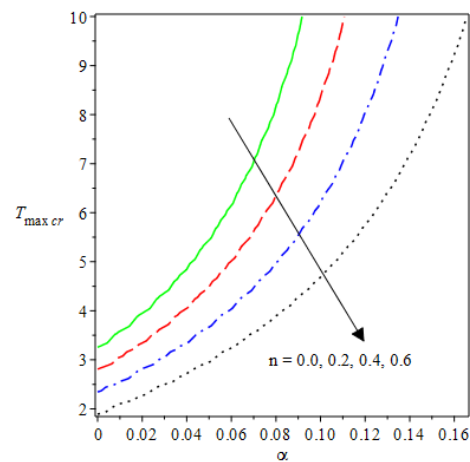
Figure 17. Branch-chain for increasing (m).

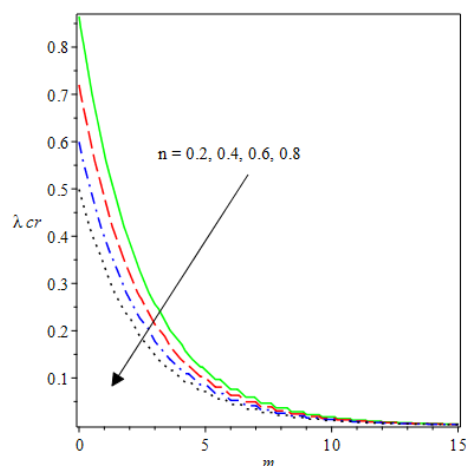**Figure 18.** Plot of $T_{max\ cr}$ versus α for rising (n).

Figure 19. Plot of λ_{cr} against m for (n).

5. Conclusions

An analysis of diffusive-oxidative high-temperature species combustion in an adiabatic concentric cylinder was conducted. The temperature distribution, bifurcation slice chain and thermal runaway were approximately analysed using the partition weighted residual scheme. The research objectives were met using this method. Hence, this method is aplicable to linear and nonlinear derivative equations in science and engineering. This study revealed that:

- The species reaction temperature distribution (T) is a monotonically enhancing function of the radius (r) with variations in thermal diffusion parameters.
- Analytical values show that T_{max} produces a concave function of (λ) with variations in the terms (α) and (m).
- The $T_{max\ cr}$ and λ_{cr} reduces as the concentric cylinder gap is increased.
- Certain parameter changes significantly influenced the heat distribution and thermal explosion under various boundary conditions.

A species reacting system with a high temperature is very useful in science and engineering for the accurate prediction of activities. This is also applicable to improvements in the efficiency of thermal system devices. However, parameters that enhance temperature distribution in a reaction system must be monitored to prevent system blowup. Further studies could evaluate the physical explosion times and transition values of a reactive species in a concentric cylinder.

Author Contributions: S.O.S.: Conceptualization, formal analysis, writing original draft, validation; S.S.O.: Formal analysis, visualization, review and editing. All authors have read and agreed to the published version of the manuscript.

Institutional Review Board Statement: The manuscript meets standards with regard to the ethics of experimentation and research integrity.

Informed Consent Statement: Not applicable.

Data Availability Statement: Not applicable.

Conflicts of Interest: There is no conflict of interest among the authors.

References

1. Makinde, O.D.; Maserumule, R.L. Thermal criticality and entropy analysis for a variable viscosity couette flow. *Phys. Scr.* **2008**, *78*, 015402.
2. Salawu, S.O.; Disu, A.B. Branch-chain criticality and explosion for a generalized thermal Oldroyd 6-constant Couette reactive fluid flow. *S. Afr. J. Chem. Eng.* **2020**, *34*, 90–96.

3.   Ajadi, S.O.; Gol'dshtein, V. Critical behaviour in a three-step reaction kinetics model. *Combust. Theory Model.* **2009**, *13*, 1–16.

4.   Boddington, T.; Gray, P.; Wake, G.C. Theory of thermal explosion with simultaneous parallel reactions I. Foundations and the one-dimensional case. *Proc. R. Soc. Lond. A* **1984**, *393*, 85–100.

5.   Boddington, T.; Feng, C.G.; Gray, P. Thermal explosion, criticality and Disapperance of criticality in systems with distributed temperature I. Arbitrary Biot number and general reactionrate laws. *Proc. R. Soc. Lond. A* **1983**, *390*, 247–264.

6.   Graham-Eagle, J.G.; Wake, G.C. The theory of thermal explosion with simultaneous parallel reactions III. Disappearance of critical behaviour with the exothermic and endothermic reactions. *Proc. R. Soc. Lond. A* **1986**, *407*, 183–198.

7.   Okoya, S.S.; Ajadi, S.O. Critical parameters for thermal condition equations. *Mech. Res. Commun.* **1999**, *26*, 363–370.

8.   Okoya, S.S. Thermal stability for a reactive viscous flow in a slab. *Mech. Res. Commun.* **2006**, *33*, 728–733.

9.   Varatharajan, B.; Williams, F.A. Chemical-kinetics description of high temperature ignition and detonation of acetylene-oxygen-diluent systems. *Combust. Flame* **2001**, *124*, 624–645.

10.   Okoya, S.S. Ignition times for a branched-chain thermal explosion chemistry with heat loss. *Toxicol. Environ. Chem.* **2009**, *91*, 905–910.

11.   Salawu, S.O.; Okoya, S.S. On criticality for a branched-chain thermal reactive-diffusion in a cylinder. *Combust. Sci. Technol.* **2020**, *192*, 1–16.

12.   Okoya, S.S. Disappearance of criticality in a branched-chain thermal explosion with heat loss. *Combust. Flame* **2006**, *144*, 410–414.

13.   Semenov, N.N. *Some Problems in Chemical Kinetics and Reactivity. Part 2*; Pergamon Press: London, UK, 1959.

14.   Zeldovich, Y.B.; Barenblatt, G.I.; Librovich, V.B.; Makhviladze, G.M. *The Mathematical Theory of Combustion and Explosions*; Consultants Bureau: New York, NY, USA, 1985.

15.   Salawu, S.O.; Kareem, R.A.; Shamshuddin, M.D.; Khan, S.U. Double exothermic reaction of viscous dissipative Oldroyd 8-constant fluid and thermal ignition in a channel. *Chem. Phys. Lett.* **2020**, *760*, 138011. *S. Afr. J. Chem. Eng.* **2020**, *34*, 90–96.

16.   Aleksandrov, E.N.; Kuznetsov, N.M.; Kozlov, S.N. Initiation of chain and thermal explosions by the reactor surface. criterion for the participation of branching chains in a thermal explosion. *Combust. Explos. Shock Waves* **2007**, *43*, 530–537.

17.   Stolin, A.M.; Bostandzhiyan, S.A.; Plotnikova, N.V. Conditions for occurence of hydrodynamic thermal explosion in flows of power-law fluid. *Heat Transf. Sov. Res.* **1978**, *10*, 86–93

18.   Okoya, S.S. Criticality effects on non-Newtonian fluids with viscous heating and thermal conductivity in cylindrical enclosure. *J. Niger. Math. Soc.* **2007**, *26*, 1–10.

19.   Kumar, M.M.J.; Satyamurty, V.V. Limiting Nusselt numbers for laminar forced convection in asymmetrically heated annuli with viscous dissipation. *Int. Commun. Heat Mass Transf.* **2011**, *38*, 923–927.

20.   Tasnim, S.H.; Mahmud, S. Mixed convection and entropy generation in a vertical annular space. *Exergy Int. J.* **2002**, *2*, 373–379.

21.   Schlichting, H. *Boundary Layer Theory*; Springer: New York, NY, USA, 2000; pp. 1–10.

22.   Machover, E.; Mastorakos, E. Numerical investigation of the stochastic behavior of light-round in annular non-premixed combustors. *Combust. Sci. Tech.* **2017**, *189*, 1467–1485.

23.   Shonhiwa, T.; Zaturski, M.B. Disappearance of criticality in thermal explosion for reactive viscous flows. *Combut. Flame* **1987**, *67*, 175–177.

24.   Okoya, S.S. Computational study of thermal influence in axial annular flow of a reactive third grade fluid with non-linear viscosity. *Alex. Engin. J.* **2019**, *58*, 401–411.

25.   Yaseen, M.; Rawat, S.K.; Kumar, M. Falkner–Skan problem for a stretching or shrinking wedge with nanoparticle aggregation. *J. Heat Transf.* **2022**, *144*, 102501.

26.   Das, S.; Chakraborty, S.; Jana, R.N.; Makinde, O.D. Mixed convective couette flow of reactive nanofluids between concentric vertical cylindrical pipes. *J. Nanofluids* **2015**, *4*, 485–493.

27.   Frank-Kamenetskii, D.A. *Diffusion and Heat Transfer in Chemical Kinetics*; Plenum Press: New York, NY, USA, 1969.

28.   Ajadi, S.O. Approximate analytic solution for critical parameters in thermal explosion problem. *Appl. Math. Comput.* **2011**, *218*, 2005–2010.

29.   Kurose, R.; Makino, H. Large eddy simulation of a solid-fuel jet flame. *Combust. Flame* **2003**, *135*, 1–16.

30.   Jha, B.K.; Samalia, A.K.; Ajibade, A.O. Transient free-convective flow of reactive viscous fluid in a vertical channel. *Int. Commun. Heat Mass Transf.* **2011**, *38*, 633–639.

31.   Li, J.; Zhong, B. Experimental investigation on heat loss and combustion in methane/ oxygen micro-tube combustor. *Appl. Therm. Eng.* **2008**, *28*, 707–716.

32.   Salawu, S.O.; Disu, A.B.; Dada, M.S. On criticality for a generalized Couette flow of a branch-chain thermal reactive third-grade fluid with Reynolds viscosity model. *Sci. World J.* **2020**, *20*, 10.

33.   Oderinu, R.A.; Aregbesola, Y.A.S. Using Laguerre's quadrature in the weighted residual method for problems with semi infinite domain. *Int. J. Pure Appl. Math.* **2012**, *75*, 95–107.

34.   Salawu, S.O.; Oderinu, R.A.; Ohaegbue, A.D. Current density and thermodynamic analysis of energy optimization for double exothermic reaction of magneto-Oldroyd 8-constant material. *J. King Saud Univ. Sci.* **2021**, *33*, 101374.